Functionalized Graphene/Ag nanoparticles Bi-layer to enhance the efficiency of polymer solar cells

Functionalized Graphene/Ag nanoparticles Bi-layer to enhance the efficiency of polymer solar cells

C F Ou[1] and Y F Chen

Department of Chemical and Materials Engineering, National Chin-Yi University of Technology, Taichung County 411, Taiwan, ROC.

[1] E-mail: oucf@ncut.edu.tw

Abstract. We prepared graphene oxide (GO) by a modified Hummer's method, and synthesized octylamine functionalized graphene (F-GNS) using long-chain octylamine as the functionalization agent. We synthesized oleic acid silver nanoparticles (OA-Ag) by the redox method. We investigated the effect of incorporating F-GNS/OA-Ag bi-layer between poly(ethylene dioxythiophene) (PEDOT)-polystyrene sulfonic acid (PSS) (PEDOT:PSS) hole transport layer (HTL) and active layer (P3HT:$PC_{71}BM$ =1:1 weight ratio) on the photovoltaic performance. The cell structure was glass/ITO/PEDOT:PSS/F-GNS/OA-Ag/P3HT: $PC_{71}BM$/Ca/Al. Four concentrations of F-GNS N-methyl pyrrolidone (NMP) solution of 0.05, 0.1, 0.3 and 0.5 mg/ml were prepared. We used the UV-Vis, SPM, FE-SEM and solar simulator to measure the absorbance, roughness, surface morphology, and power conversion efficiency (PCE), respectively. From these results, we found that the short circuit current density(J_{sc}) and PCE of the cells with F-GNS/OA-Ag are always higher than those of cell without F-GNS/OA-Ag. The cell with 0.1 mg/ml F-GNS/OA-Ag bi-layer had the highest J_{sc} of 8.51 mA/cm^2, an increase of 32% and the highest PCE of 2.96%, an increase of 28% compared to the reference cell. These improvements were due to the high carrier mobility of graphene.

1. Introduction

Polymer solar cells have attracted considerable attention due to their potential as a renewable, alternative source of electricity and their preference in low cost, light weight, flexible and easy processing conditions as compared to the conventional inorganic solar cell [1]. Solution-processable polymer bulk heterojunction (BHJ) solar cells have potential as a cost-efficient power source [2-3]. In conventional BHJ solar cells, poly(3-hexylthiophene)(P3HT) as electron donor and [6,6]-phenyl-C_{71} butyric acid methyl ester ($PC_{71}BM$) as electron acceptor blend layer is sand-wiched between a transparent anode and a low work-function metal cathode such as Ca/Al or LiF/Al. Water-soluble poly(3,4-ethylenedioxythiophene):poly(styrene-sulfonate) (PEDOT:PSS) has been widely used as an appropriate hole transport layer (HTL) for more efficient hole collection via alignment of work functions of P3HT and transparent ITO anode as well as improvement of contact between active layer and transparent anode by minimizing the detrimental effects of ITO roughness [4].

Graphene, an atomic thin layer with sp^2-hybridized carbon atoms tightly packed into a two-dimensional honeycomb structure, is considered as a new material used in polymer solar cells due to its novel properties. Graphene exhibits a considerable number of new and sometimes mysterious optical and electronic effects that have not been observed in other materials, such as zero-band-gap semi-conductivity with a high carrier mobility, high optical transparency and high tensile strength [5]. Various chemical synthetic methods are used to obtain graphene for basic studies and industrial

applications [6]. Additionally, derivatives of graphene, such as graphene oxide and reduced graphene oxide, are being widely investigated from the point of view of primary and practical applications [7]. Polymer solar cells that contain graphene are investigated in three aspects: (i) as the additives to the donor or donor-acceptor material in the BHJ organic photovoltaic cells [8], (ii) as a transparent conductive electrode (anode or cathode) [9] and (iii) as a segregated layer for organic photovoltaic cells [10]. Recently, graphene decorated with various inorganic nanoparticles, such as Au, Pt, Ag, TiO_2 and ZnO [11-12], among which Ag nanocomposites are good candidates for electronics, optics, electrochemistry and catalyst [11-12]. The functionalized graphene (F-GNS) was synthesized from GO using long-chain octylamine as the functionalization agent. The F-GNS exhibits good distribution in solvent. In this paper, we investigated the effect of incorporating F-GNS/OA-Ag bi-layer between PEDOT:PSS and active layer on the characteristics of polymer solar cell.

2. Experimental

The ITO substrates (15 ohm/cm^2) were bought from Lumtec Corp. Graphites powder (~325 mesh) were purchased from Alfa Aesar. Graphite oxide (GO) was produced via a modified Hummer's method [11], using graphite as raw material and $KMnO_4$, $KClO_4$, $NaNO_3$ and 98% H_2SO_4 as oxidants. The Graphene/Ag nanoparticles were prepared in one step reaction [13]. The 1.0 mg/ml GO water solution was prepared and stirred by ultrasonication for 1 hr. The 1.0 mg/ml octylamine alcohol solution was prepared. The GO solution and octylamine solution were mixed and stirred at 60 °C for 10 hr. Then the reduced agent of hydrazine hydrate was added and stirred for 2 hr. The solution was centrifuged and washed with methanol and pure water and the F-GNS was obtained. Four concentrations of F-GNS N-methyl pyrrolidone (NMP) solution of 0.05, 0.1, 0.3 and 0.5 mg/ml were prepared. The OA-Ag (oleic acid silver) particles was synthesized using silver nitrate, oleic acid and sodium borohydride.

ITO substrates were cleaned with a special detergent followed by ultrasonication in acetone and isopropyl alcohol and then kept in an100 °C oven for 30 min. Before the preparation of hole transport layer (HTL), all substrates were treated with UV/O_3 for 10 min to increase wettability of ITO surface. The device structure, PEDOT:PSS (Baytron P AI 4083) HTL with a thickness of 40 nm was spin-coated on to the UV/O_3-treated ITO/glass substrates followed by annealing at 120 °C for 10 min. The F-GNS NMP solution was spin-coated at 6000 rpm on the HTL layer and dried at 150 °C for 10 min, then 0.025 g/ml OA-Ag 1,2-dichlorobenzene solution was spin-coated at 6000 rpm on the F-GNS layer and dried at 150 °C for 10 min. The active layer material (P3HT:$PC_{71}BM$=1:1 weight ratio) was dissolved in o-dichlorobenze (o-DCB) and placed on a hot-plate at temperature 70 °C, rotation speed 150 rpm for 24 h. Active layers were spin-coated on F-GNS/OA-Ag bi-layer at 500 rpm for 60 s using o-DCB solution containing a 25 mg/mL of P3HT(Rieke Metals) and a 25 mg/mL of $PC_{71}BM$ (Nano-C). Then, to obtain highly ordered active layer, the active layer coated substrates were kept in a glass jar at room temperature to evaporate o-DCB solvent slowly for 2 h in an N_2-filled glove box, followed by annealing at 150 °C for 30 min inside the glovebox. Finally, cathode electrodes composed of Ca (50 nm)/Al (90 nm) with an area of 10 mm^2 were deposited using a thermal evaporator in vacuum with a pressure of 10^{-6} Torr. Figure 1 shows the schematic diagram of the solar cell.

Performances of the solar cell were obtained from the current-density-voltage characteristics under solar stimulated irradiation (AM 1.5). The solar simulator used for this work was 2400 digital source meter (Keithley, USA) under illumination by a Class A sunlight simulator of 100 mw/cm^2 (91160A, AM 1.5 Oriel, Newport Corporation, USA), which was equipped with an AM 1.5 G filter (81088A, Oriel, Newport Corporation, USA). The properties of $V_{oc,}$ $J_{sc,}$ FF, and PCE reported here represents an average value of six measurements for each sample.

The optical properties of were investigated via. UV–vis spectrophotometer with a Cary 100 conc. The photoluminescence (PL) was measured using Shimadzu RF-5301PC. The surface morphologies were measured by SPM using a Digital instrument NS3a operated in tapping mode with a silicon antilever. The morphology of the F-GNS was obtained by SEM observation using a JSM-6360 scanning electron microscope (Jeol).

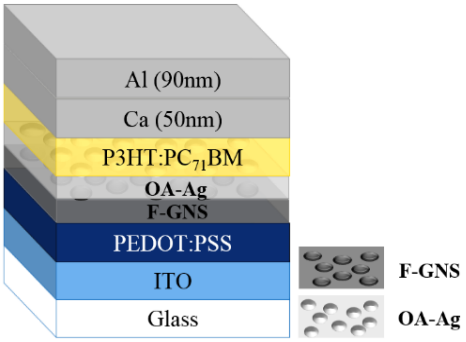

Figure 1. Schematic diagram of the solar cell.

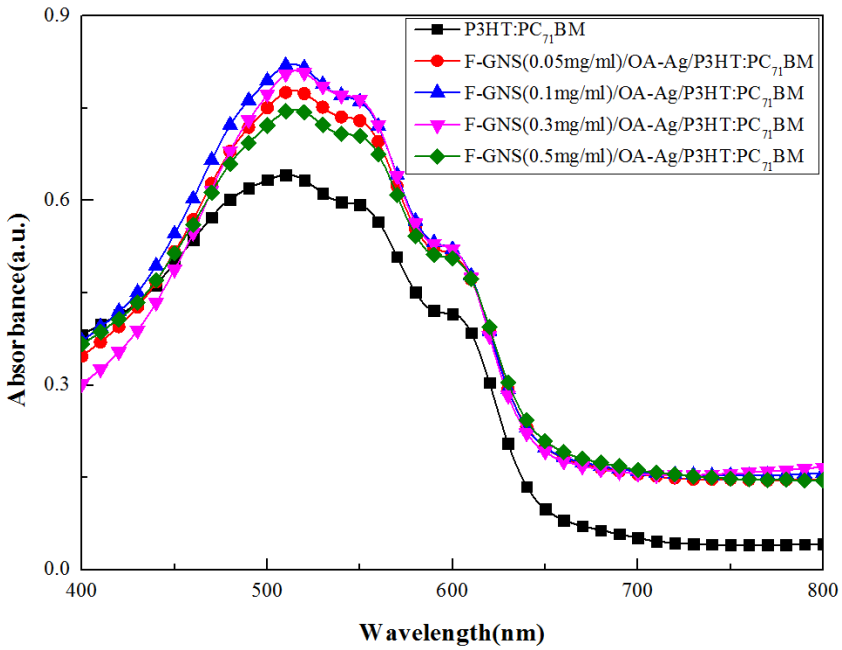

Figure 2. The UV–vis spectra of photovoltaic device.

3. Results and discussions

Figure 2 shows UV-vis absorption spectra of annealed film with different concentrations of F-GNS layer. As the F-GNS/OA-Ag bi-layer was incorporated between PEDOT hole transport layer and active layer, absorption peak of P3HT (~525nm) increases and broadens, besides showing blue-shift. This tendence depends on the concentrations of F-GNS. The cell with F-GNS/OA-Ag bi-layer exhibited higher absorbance than that of cell without F-GNS/OA-Ag, as shown in Table 1. The cell with 0.1 mg/ml F-GNS/OA-Ag bi-layer had the highest absorbance of 0.82 and an increase of 28%, compared to the reference cell without F-GNS/OA-Ag bi-layer. The PL curves of photovoltaic device were shown in Figure 3. The quenching areas ratio of photoluminescence of four F-GNS concentrations (0.05, 0.1, 0.3 and 0.5 mg/ml) were 76%, 79%, 78% and 75%, respectively (Table 2). The cell with 0.1 mg/ml F-GNS/OA-Ag bi-layer exhibited the highest quenching areas ratio of photoluminescence. Figure 4 shows the SPM of photovoltaic device with different F-GNS concentrations. The root mean square roughness (Rq) of F-GNS layer (0.05, 0.1, 0.3 and 0.5 mg/ml) were 13.6 nm, 9.25 nm, 10.1 nm and 13.2 nm, respectively (Table 3). The cell with 0.1 mg/ml F-GNS layer exhibited the smallest roughness. Figure 5 shows the SEM images of F-GNS layer. The size of

F-GNS increased with increasing the F-GNS concentrations. The cell with 0.1 mg/ml F-GNS layer had the best distribution in the layer.

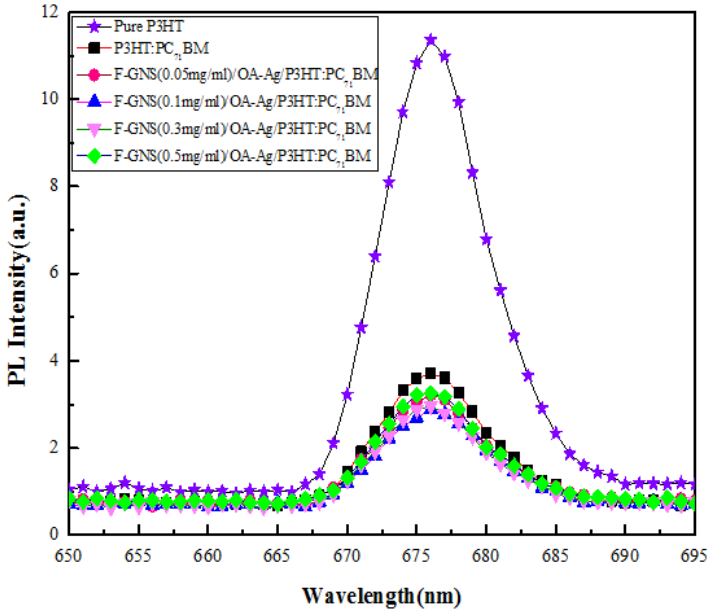

Figure 3. The PL curves of photovoltaic device.

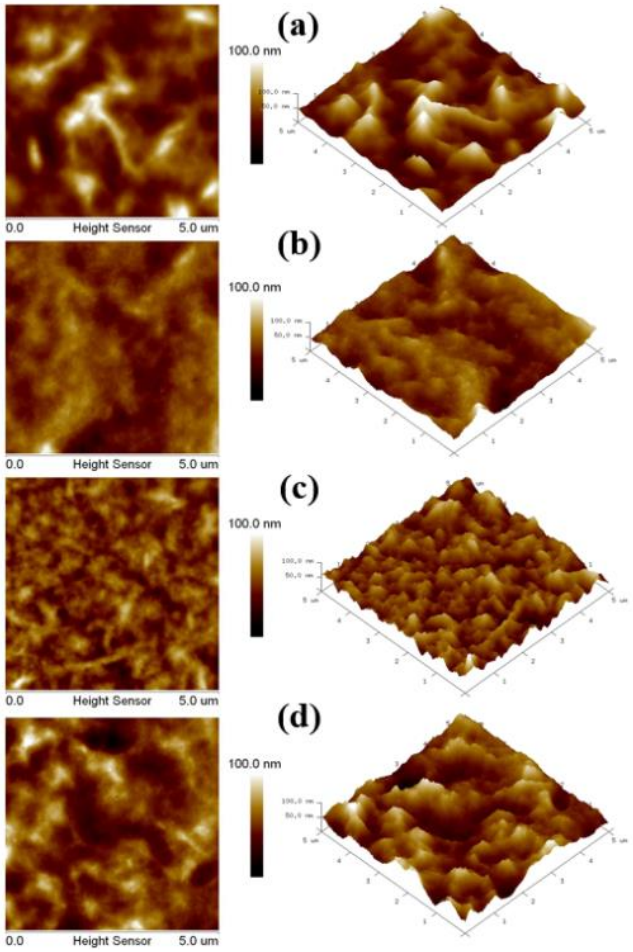

Figure 4. SPM images of photovoltaic device with (a)0.05 mg/ml (b)0.1 mg/ml (c)0.3 mg/ml (d)0.5 mg/ml F-GNS layer.

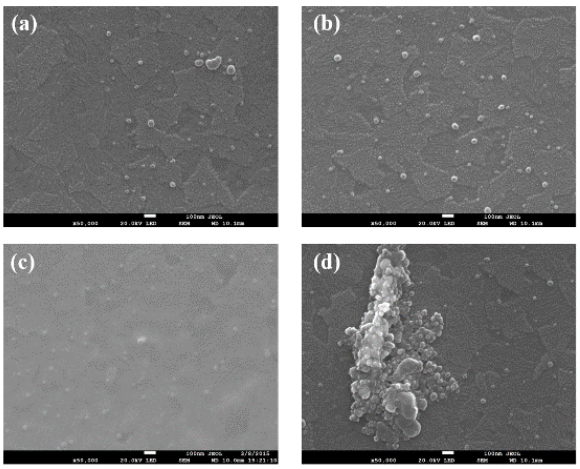

Figure 5. SEM images of F-GNS layer (a)0.05 mg/ml (b)0.1 mg/ml (c)0.3 mg/ml (d)0.5 mg/ml (x30000).

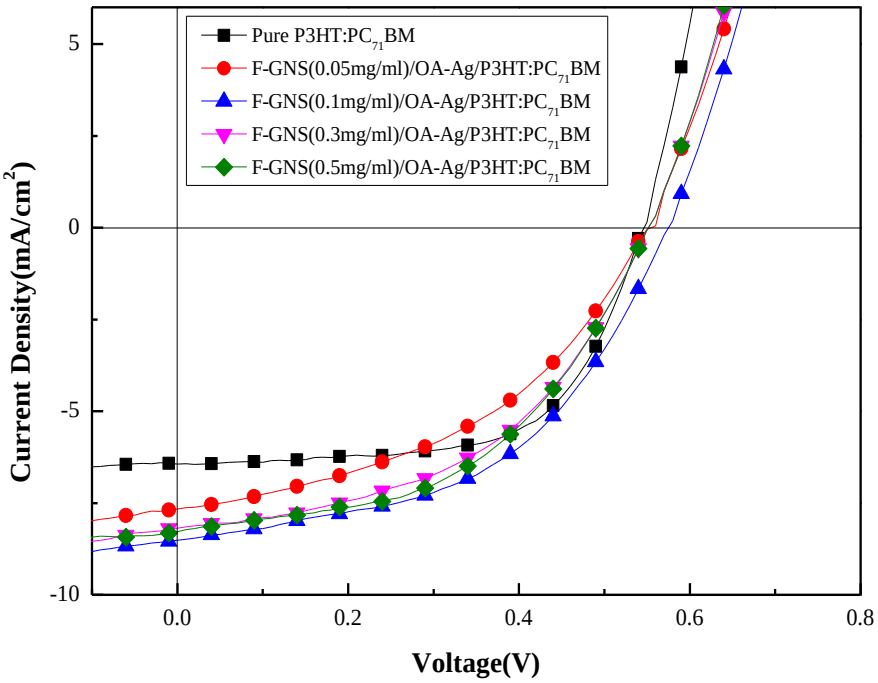

Figure 6. The J-V curves of photovoltaic devices.

Table 1. The absorbance of photovoltaic device.

composition	Absorbance (a.u.)
Reference	0.64
F-GNS(0.05mg/ml)/OA-Ag	0.78
F-GNS(0.1mg/ml)/OA-Ag	0.82
F-GNS(0.3mg/ml)/OA-Ag	0.81
F-GNS(0.5mg/ml)/OA-Ag	0.75

Table 2. The quenching areas ratio of photovoltaic device.

composition	quenching areas ratio (%)
Reference	70
F-GNS(0.05mg/ml)/OA-Ag	76
F-GNS(0.1mg/ml)/OA-Ag	79
F-GNS(0.3mg/ml)/OA-Ag	78
F-GNS(0.5mg/ml)/OA-Ag	75

Table 3. The roughness of photovoltaic devices.

composition	Rq(nm)
Reference	16.60
F-GNS(0.05 mg/ml)/OA-Ag	13.60
F-GNS(0.1 mg/ml)/OA-Ag	9.25
F-GNS(0.3 mg/ml)/OA-Ag	10.10
F-GNS(0.5 mg/ml)/OA-Ag	13.20

Table 4. Photovoltaic performance of photovoltaic devices.

composition	V_{oc} (V)	J_{sc} (mA/cm^2)	FF	PCE (%)
Reference	0.55	6.44	0.62	2.32
F-GNS(0.05 mg/ml)/OA-Ag	0.55	7.67	0.44	2.65
F-GNS(0.1 mg/ml)/OA-Ag	0.58	8.51	0.49	2.96
F-GNS(0.3 mg/ml)/OA-Ag	0.55	8.19	0.48	2.70
F-GNS(0.5 mg/ml)/OA-Ag	0.55	8.28	0.49	2.57

The current-voltage plots of the devices are shown in Figure 6. The $J_{sc,}$ open-circuit voltage (V_{oc}), fill factor (FF), and PCE values for each set of devices are summarized in Table 4. It can be seen that the reference device without F-GNS/OA-Ag bi-layer exhibited J_{sc} of 6.44 mA/cm^2 and PCE of 2.32%. The insertion of F-GNS/OA-Ag bi-layer between PEDOT:PSS and active layer results in a substantial increase in J_{sc} and PCE. The device with 0.1 mg/ml F-GNS/OA-Ag bi-layer had the highest J_{sc} of 8.51 mA/cm^2, an increase of 32% and PCE of 2.96%, an increase of 28% compared to the reference cell. This improvement in performance reveals that the hole transport path becomes more well-defined and charge transport properties of active layer was improved by the insertion of F-GNS/OA-Ag bi-layer between HTL and active layer. The device with 0.1 mg/ml F-GNS/OA-Ag bi-layer exhibited the highest absorbance and quenching areas ratio, the smallest roughness and the best distribution of F-GNS among all of the samples. These results induced that the cell with 0.1 mg/ml F-GNS/OA-Ag bi-layer exhibited the highest J_{sc} and PCE.

4. Conclusions

We have successfully inserted F-GNS/OA-Ag bi-layer between PEDOT:PSS HTL and P3HT: $PC_{71}BM$ (1:1) active layer. The insertion increased J_{sc} and PCE of device. This improvement in performance is due to an extension of the excitions dissociation area and to faster hole transport through the graphene or Ag nanoparticles leading to an enhancement in the PCE. The device with 0.1 mg/ml F-GNS/OA-Ag bi-layers had the highest J_{sc} of 8.51 mA/cm^2, an increase of 32% and PCE of 2.96%, an increase of 28%. The reason was that the device with 0.1 mg/ml F-GNS/OA-Ag bi-layers had the highest absorbance in UV-vis absorption and quenching areas ratio of photoluminescence, the highest uniform distribution and the smallest roughness.

References

[1] Mayer A C, Scully S R, Hardin B E, Rowell M W and McGehee M D 2007 Polymer-Based Solar Cells *Mater Today* vol **10** P 28–33

[2] Liang Y Y, Feng D, Wu Y, Tsai S T, Li G, Ray C and Yu L 2009 Highly Efficient Solar Cell Polymers Developed via Fine-Tuning of Structural and Electronic Properties *Journal of the American Chemical Society* vol **131** P 7792–7799

[3] Meyer J, Khalandovsky R, G orrn P and Kahn A 2011 MoO_3 Films Spin-Coated from a Nano Particle Suspension for Efficient Hole-Injection Inorganic Electronics *Advanced Materials* vol **23** P 70–73

[4] Bisoyi H K andKumar S, 2011 Carbon-Based Liquid Crystals: Art and Scienc *Liq Cryst* vol **38** P 1427-1449

[5] Allen M J, Tung V C and Kaner R B 2010 Honeycomb Carbon: A Review of Graphene *Chem Rev* vol **110** P 132-145

[6] Dreyer D R, Park S, Bielawski C W and Ruoff R S 2010 The Chemistry of Graphene Oxide *Chem Soc Rev* vol **39** P 228-240

[7] Yu D, Park K, Durstock M and Dai L 2011 Fullerene-Grafted Graphene for Efficient Bulk Heterojunction Polymer Photovoltaic Devices *The Journal of Physical Chemistry Letters* vol **2** P 1113-1118

[8] Hsu C L, Lin C T, Huang J H, Chu C W, Wei K H and Li L J 2012 Layer-by-Layer Graphene/Tcnq Stacked Films as Conducting Anodes for Organic Solar Cells *ACS Nano*, vol **6** P 5031-5039

[9] Ryu M S and Jang J 2011 Effect of Solution Processed Graphene Oxide/Nickel Oxide Bi-layer on Cell Performance of Bulk-Heterojunction Organic Photovoltaic *Sol Energy Mater Sol Cell,* vol **95** P 2893-2896

[10] Yang Y and Liu T X 2011 Fabrication and Characterization of Graphene Oxide/Zinc Oxide Nanorods Hybrid *Applied Surface Science* vol **257** P 8950-8954

[11] Wang H L, Robinson J T, Li X L and Dai H J 2009 Solvothermal Reduction of Chemically Exfoliated Graphene Sheets *Journal of the American Chemical Society* vol **131** P 9910-9911

[12] Yuan W H, Gu Y J and Li L 2012 Green Synthesis of Graphene/Ag Nanocomposites *Applied Surface Science* vol **261** P 753-758

[13] Li J and Liu C Y 2010 Ag/graphene heterostructures: synthesis, characterization and optical properties *European Journal of Inorganic Chemistry* vol **10** P 1244-1248